High resolution bead technique measurements and multipole analysis

A.M.Porcellato, M.Cavenago and M.Morvillo, INFN-LNL ,Legnaro, Italy

Abstract

The bead perturbation of the frequency in a resonant cavity provides accurate mapping of electrical field intensity. The bead diameter is 3 mm, to improve the spatial resolution, which makes the measure extremely sensitive to resonator thermal drifts. A large insulated test chamber was designed and installed in our laboratory to limit the cavity temperature changes to about 0.00001 K/s. The better stability and a more stable electronic equipment allowed to improve the frequency resolution to 1 Hz. The data are analysed to determine the multipole components of the electrical field along the beam axis and to compare them with the results obtained by well-known codes. Practical advantages of the bead technique method, i.e. unbiasness, sensitivity to manufacture errors and shape resolution, are outlined.

1 INTRODUCTION

The radiofrequency fields multipolar components on the beam path in a QWR (Quarter Wave Resonator) were estimated by perturbation technique in a previous work [1]. A map of the square of the electrical field in the beam hole was obtained from of the resonant frequency shifts produced by a spherical bead travelling on and at suitable distances from the beam axis. From such a data it was possible to determine the electrical field component, thank to a Fourier-Bessel decomposition and reconstruction of the quasi-static potential [2]; impulse transferred to beam was then easily obtained. The result precision was limited by the resonator thermal drift during data acquisition, and by the fact that a small bead is necessary to have a satisfying spatial resolution (1-2 mm). A 3 mm teflon sphere produces a maximum frequency shift of about 400 Hz while for ALPI medium beta resonator the resonant frequency change is 2.7 kHz/K . The thermal drift was reduced to $4\times\ 10^{-6}$K /s inserting the resonator in a suitably built chamber, with a large thermal capacity provided by 500 liter of water and insulation provided by plastic walls; active stabilization methods were not possible, since they usually give a sawtooth variation of frequency. This thermal stability and a better control of the frequency shift measurement, allowed a resolution $F = 1$ Hz; accuracy and precision of the dipole and quadrupole coefficient values improved. Data analysis is greatly simplified thanks to the higher resolution of data, since the main problem encountered before was to discriminate peak from background regions, where frequency slowly drifts.

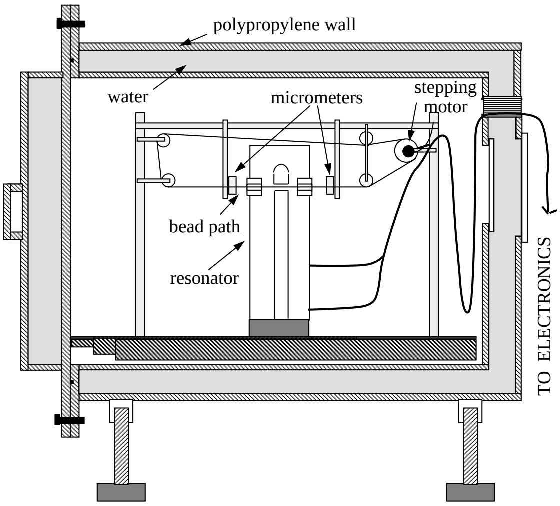

Figure 1: The cavity

2 THE THERMOSTATIC CHAMBER

The bead travel necessary to sample the QWR beam path is about 24 cm, the inner QWR diameter being 18 cm and three more cm left on the sides to determine the residual thermal drift. Each path records 256 data points to obtain a spatial resolution comparable to the bead radius and to use the Fast Fourier Transform for data analysis. The frequency shift measurement at each point needs 2 seconds, 1 second being the frequency meter reading time at 1 Hz resolution and 1 second being the time to dump the oscillation due to the bead motion. Consequently the acquisition time is 512 seconds per scan. The thermal stability required to limit the resonant frequency shift to a value lower than a 10 % of the effect to be measured (about 400 Hz) is $dT/dt\ =\ 3\times\ 10^{-5}$ K /s, where T is the average temperature of the copper cavity.

Let us discuss the thermalization times between an unprotected cavity and a generic room in some detail; estimate of thermalization times between the whole thermostatic chamber and the room or between a cavity and the thermostatic chamber which contains it are similar.

The resonator under test is built in copper and weights 30 Kg, so the thermal capacity C_t is 11500 J/K . The thermal exchange between resonator and environment is mainly by convention, natural or forced. The heat flux (dq/dt) is given by:

$$dq/dt = a\ S\ (T_c - T_a) \tag{1}$$

where a is the convention coefficient, S is the exchange surface (0.38 m^2) and $(T_c\ -\ T_a)$ is the difference in temperature between cavity and environment. The convention coefficient is given by $a = \lambda$ Nu$/d$ where λ is the air thermal conductivity (0.02624W/m/K at room temperature), d is the resonator outer diameter (20 cm) and Nu is the Nusset number Nu $= C$ Re^n, with Re the well-known Reynolds number and C and n suitable coefficients, depending on the Re value and on the geometry. In our case, assuming an air velocity $v = 1$ m/s, we have $C = 174$, $n = 0.618$ and Re $= 12700$ at room temperature. That gives Nu$= 6\times 10^5$ and consequently $a = 7.91$ W m^{-2}K^{-1}.

The difference in temperature between cavity and environment at the time t decays exponentially as:

$$T_c - T_a = c_1 \exp[-t/\tau] \tag{3}$$

where the relaxation time τ is $\tau = C_t/(aS)$, that is 4000 seconds for our resonator.

A difference of 1 K (a reasonable estimate of fluctuation or transients) between cavity and environments gives an unacceptably large heat flux $dq/dt = 3$ W/K, which produces a thermal drift of 0.16 K in 512 sec and consequently a 430 Hz shift in resonant frequency, larger than the effect we want to measure. To obtain the required stability the thermal flux on the resonator must be limited

$$dq/dt = C_t\ (dT/dt) = 0.34\text{W} \tag{4}$$

so that the thermal fluctuation during a test $T_c - T_a$ is less than 0.1 K . It is impossible to reach such a stability level by active method. The resonator was then inserted in a high thermal capacity chamber that insulates the resonator, filtering the thermal fluctuation from the outside. The realised device is sketched in fig. 1. It is a double wall box built in polypropylene two cm thick, weighting about 500 kg. The hollow space contains about 500 litres water. The inner useful space is 100x80x140 cm^3. One of the side face is flanged and it is closed by a polypropylene door hinged on the side. It is fixed on an airtight rubber gasket, located on the flange, by means of screws. On the opposite side there is a double window and a cable crossing hole.To avoid direct sun radiation an isolating aluminised sponge covers the chamber. An aluminium plate that supports the resonator and the bead movements. can be completely extracted from the chamber.

In this case the device thermal capacity is 3.3×10^6 J/K. The heat exchange coefficient, computed in the previous indicated condition (air speed 1 m/s), is about 25 W/K and the thermalization time with the environment is about 28 hours. An external temperature change of 1 K causes a thermal drift in the resonant frequency of 13 Hz in a scan.

The bead is carried by a thread (0.2 mm thick) along the z axis, by a stepping motor driven pulley. Four more pulleys maintain the thread in a close loop and allow to adjust the tension. The thread position can be changed by two couples of micrometers that can move the thread supports on the xy plane. These have a 20 mm hole. A 19.8 mm rod was used to align these holes to the cavity beam hole.

3 FREQUENCY MEASUREMENT

The bead motion on the z axis and the frequency measurements are computer controlled [3]. It is possible to set the frequency meter sensitivity, the step number, the starting time, the acquisition cycles, the direction of motion. For

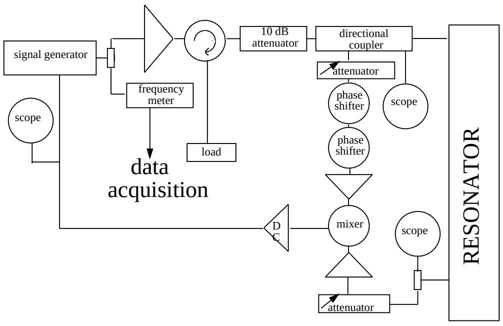

Figure 1: The circuit

measuring on axis and off axis, the position of the thread on the yz plane must be changed opening the chamber door. Repositioning requires about 5 minutes, but the following data acquisitions have to be delayed of at least 1 hour to recover the thermal perturbation. The set-up for the frequency shift measurement is presented in fig.2. The phase shift θ between the driving signal and the resonator pick-up signal, produced by the bead, is converted into a voltage by a mixer ($V = K_m\theta$ with $K_m = 0.297$ V/rad), and after a suitable amplification modulates a voltage controlled stabilized oscillator. The phase shifters allow to adjust the delay between the two signals in order to zero the voltage output, at a defined resonance. The measured frequency shift is related to the change on the resonator frequency f_r by $\delta f = C(f_r - f_o)$ where f_o is generator central frequency and the closed loop gain is

$$C = QBK_m/(f_o + BQK_m) \tag{5}$$

with Q the resonator loaded quality factor (8000) and the feedback gain $B = A(dF/dV)$. Here dF/dV is the change in generator frequency $f_g - f_o$ per a unit voltage (set at 100 kHz/V) and A is the gain of the DC amplifier (1000). The product QBK_m resulted $(2.38\pm 0.14)\times 10^{11}\pm$ Hz/rad, that makes the error on C equal to 3.6×10^{-4} and practically negligible. Such a strong feedback was possible using DC amplifier isolated by the power line, with a low offset (10μV/K). The DC amplifier roll-off frequency that maximizes the possible gain without starting auto-oscillation in the feedback loop was 300 Hz at 6 dB.

Note that the feedback system compensates for every change on DC amplifier gain and offset, but not the residual error, due to the change in electric length difference between the two circuit branches up to the mixer inputs. The produced phase shift can not be separated by the one produced by the resonator itself (5×10^{-5} rad/Hz) in our measure of δf . The measures are then performed during night without people around and after that the electronic was stabilised to minimise such an error.

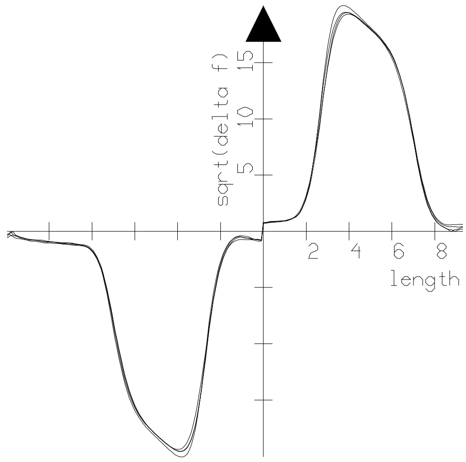

Figure 3 : Profiles of $\sqrt{\delta f}$ in Hz$^{1/2}$ versus z for different x, y, with signs so that they are proportional to E_z.

4 IMPROVEMENTS IN DATA ANALYSIS

Note that from eq. 3 we can expect that a parabolic background will be more appropriate than a linear one, as we assumed in [2]. After subtracting this background, data were analyzed as the previous $F = 10$ Hz resolution data by TOLLNL, confirming previous results for deflection coefficient (and other quantities of primary interest for beam dynamics as transit time factor and quadrupole focusing). They are not in complete agreement with 3d numerical simulation, that we performed with the well-known code MAFIA [5]. Simulation problem were the limited number of mesh points and interpolation. For brevity sake, see figs. 6,8,10 in Ref [2] for still valid results in beam dynamics.

It can be noted that while both data reduction [2] and 3d simulations assumed exact reflection symmetry on xy and xz planes for speeding up programming and/or geometry input, the actual measured data are sensitive to mechanical imperfection and coupler position perturbations. In perspective, some assumption of [2] may be relaxed making possible to measure the electrical effect of cavity imperfection directly.

Let us discuss some techniques in subtracting the parabolic background from the peaks representing the useful E_z field of a QWR; the difficulty is that we can not postulate any particular shape of the peaks. The distinctive feature of background points is then the facts of lying closely to a line (or a parabola), within a quantity D (proportional to the expected standard deviation σ_f of f measurement at each point, which is $F/2\sqrt{3} \cong 0.3$ Hz), while peak points are far. Therefore the additional unlikelihood of being the background line is zero when this line passes for the point considered, increases quadratically for small deviations and smoothly saturates to a constant when deviations are much larger than D ; that give us the modified chi-square

$$\chi_m^2(a,b,c) = \sum_{i=1}^{N} 1 - \frac{D^2}{D^2 + (f_i - (a + bz_i + cz_i^2))^2} \quad (6)$$

where f_i are the measured data at position z_i; the value $N - \chi_m^2$ tells how many points belongs to background and is a measure of success in background extraction. Since eq. (6) does not require different weights for points (or any form of cuts of data), it has the theoric advantage of being unbiased and the practical advantage of not requiring judicious input of cuts from the user. Well proven packages [4] can be used in minimizing (6). It must be noted the initial starting point choice is even more critical than it is for the usual chi-square; by a physical analogy, chi-square is attracted by every point, while modified chi-square is attracted by the only points within D from the guessed line. It is of practical advantage to start with $D = 1.6$ Hz to be reduced to $D = 0.8$ Hz; in case this search fails, a time consuming initial scan of a, b, c is used.

Result from background subtraction (with centering and zero leveling) can be seen in Fig 3, to be compared with fig 3 in Ref [2], where a much higher noise level is apparent; after TOLLNL analysis that noise was cut away, so that Fig 5 of Ref [2] is more similar to present Fig. 3. Note that systematic asymmetry of f perturbation is now visible, and what is even more interesting, it does reduce and change shape when a copper bead is used. On the contrary, this asymmetry does not depend from bead travelling towards positive or negative z.

5 ACKNOWLEDGEMENTS

The authors thank L.Bertazzo, A.Dainese, L.Tiso for technical support in chamber construction, L.Boscagli, G.Casa and D.Carlucci for help with measurements.

6 REFERENCES

[1] A.M. Porcellato, A.Battistella, G.Bisoffi, M.Cavenago, *Conference Record of the IEEE 1991 Part. Acc. Conf.* vol4, p.2438-2440 (1991), (ed. IEEE Service Center, Piscataway).

[2] M. Cavenago, *Nucl. Instr. Meth.* , **A 311**,19 (1992)

[3] A.Porcellato, A.Battistella, S.Marigo, “Automation of the cavity parameter measurements”, in (P.Marin, P.Mandrillon, eds.), *Proceedings of the 2nd European Particle Accelerator Conference 90*, vol. 2, pp. 1109-1111, Editions Frontieres, Gif-sur-Yvette, 1990

[4] F.James, ”Minuit”, CERN Program Library Long Writeup D506

[5] T. Weiland, *U.R.S.I. International Symposium on Electromagnetic Theory*, Budapest, Hungary, Proceedings Part B, pp. 537-542, 1986.